

Effects of Orientation on Critical Heat Flux From Chip Arrays During Flow Boiling

C. O. Gersey

I. Mudawar

Assistant Professor and Director.

Boiling and Two-Phase Flow Laboratory,
School of Mechanical Engineering,
Purdue University,
West Lafayette, IN 47907

Boiling experiments were performed with FC-72 on a series of nine in-line simulated microelectronic chips in a flow channel to ascertain the effects of channel orientation on critical heat flux (CHF). The simulated chips, measuring 10 mm × 10 mm, were flush-mounted to one wall of a 20 mm × 5 mm flow channel. The channel was rotated in increments of 45 degrees through 360 degrees such that the chips were subjected to coolant in upflow, downflow, or horizontal flow with the chips on the top or bottom walls of the channel with respect to gravity. Flow velocity was varied between 13 and 400 cm/s for subcoolings of 3, 14, 25, and 36°C and an inlet pressure of 1.36 bar. While changes in angle of orientation produced insignificant variations in the single-phase heat transfer coefficient, these changes had considerable effects on the boiling pattern in the flow channel and on CHF for velocities below 200 cm/s, with some chips reaching CHF at fluxes as low as 18 percent of those corresponding to vertical upflow. Increased subcooling was found to slightly dampen this adverse effect of orientation. The highest CHF values were measured with near vertical upflow and/or upward-facing chips, while the lowest values were measured with near vertical downflow and/or downward-facing chips. These variations in CHF were attributed to differences in flow boiling regime and vapor layer development on the surfaces of the chips between the different orientations. The results of the present study reveal that, while some flexibility is available in the packaging of multi-chip modules in a two-phase cooling system, some orientations should always be avoided.

Introduction

The continued miniaturizing of electronic components over the past decade has caused the power dissipation at the chip and circuit board levels to increase drastically. In the near future, power dissipation per chip could reach 100 W/cm² (Simons, 1987). Much attention has been focused toward direct immersion cooling with phase change as a means of dissipating high heat fluxes while maintaining the chip at an acceptable operating temperature. Numerous researchers have studied either direct immersion cooling of simulated microelectronic chips in pool boiling (Nakayama et al., 1984; Park and Bergles, 1988; Park et al., 1990; Anderson and Mudawar, 1989; Mudawar and Anderson, 1989a,b) or in forced-convection boiling in a flow channel. Invariably, the channel configurations previously studied were either vertical with coolant upflow (Maddox and Mudawar, 1989; Mudawar and Maddox, 1989; McGillis et al., 1991; Willingham et al., 1991; Willingham and Mudawar, 1992), or horizontal with the simulated chip surfaces upwards facing with respect to gravity (Lee and Simon, 1989;

Samant and Simon, 1989). Currently, the electronic packaging industry lacks an understanding of the effects of orientation on forced-convection boiling heat transfer from multi-chip circuit boards.

Several researchers have tested the effect of surface orientation in pool boiling. Figure 1(a) details the three cardinal angles typically tested in pool boiling: 90 degrees (horizontal, upward facing surface), 0 degrees (vertical), and -90 degrees (horizontal, downward-facing surface). Notably, Nishikawa et al. (1983) studied pool boiling of water on a copper surface varying the angle of inclination from 90 degrees to -85 degrees. For low heat fluxes, decreasing the angle of inclination from 90 to -85 degrees enhanced boiling, resulting in a lower wall temperature for a given heat flux. For angles between 90 and -30 degrees, the bubbles swept along the heated surface agitating and disrupting the superheated liquid layer, causing better mixing with the bulk fluid, which reduced the wall temperature. For angles between -60 and -85, heat transfer was augmented by the evaporation of a thin liquid film trapped between the elongated bubbles and the surface even though there was not much bubble agitation. Nishikawa et al. measured no effect of orientation on heat transfer at high heat fluxes, and they attributed this observation to the vigorous effusion of vapor promoting efficient mixing with the bulk liquid at all orientations.

Contributed by the Electrical and Electronic Packaging Division and presented at the ASME/JSME Joint Conference on Electronic Packaging, Milpitas, Calif., April 9-12, 1992 of THE AMERICAN SOCIETY OF MECHANICAL ENGINEERS. Manuscript received by the EEPD January 10, 1992; revised manuscript received April 23, 1992. Associate Technical Editor: B. G. Sammakia.

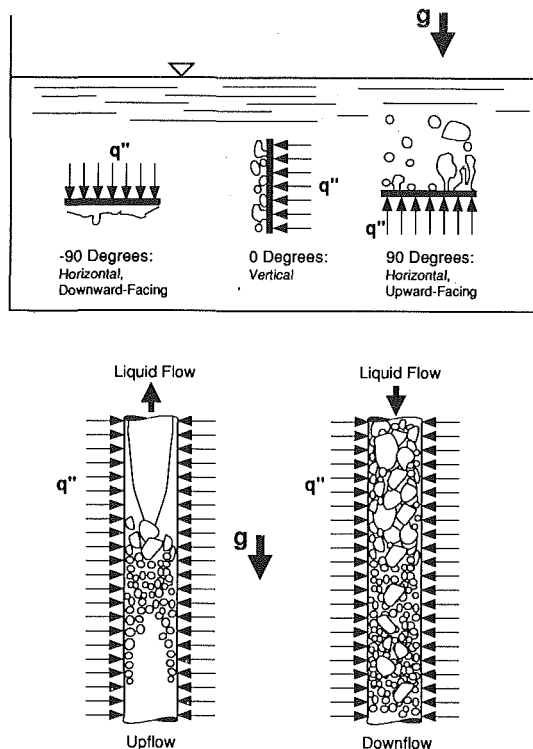


Fig. 1 Illustration of orientation nomenclature used in (a) pool boiling and (b) forced-convection boiling

In his studies on pool boiling of Freon-11 on a copper surface for angles between 90 and -60 degrees, Chen (1978) observed an enhancement similar to that reported by Nishikawa et al. for low heat fluxes but, unlike Nishikawa et al., he found the same trend to persist at high heat fluxes. By combining a balance of the surface tension and buoyancy forces on a growing bubble with the thermodynamic equilibrium criterion for the wall superheat required to grow a bubble from a cavity, Chen showed that the wall superheat decreased as the angle increased between 0 and 90 degrees. For angles between 0 and -60 degrees, Chen measured a continued decrease in ΔT_w which he attributed to bubble agitation of the superheated liquid layer as the bubble moved along the surface, and to premature shearing of growing bubbles by other moving bubbles. When the surface was rotated past -60 degrees, the bubbles no longer migrated away from the surface thus inhibiting mixing and the replenishment of liquid to the surface, which increased the wall temperature.

In the pool boiling of isopropyl alcohol, Githinji and Sabersky (1963) found the boiling curve and CHF for $\theta = 0$ and $\theta = 90$ degree orientations were close to each other, with the vertical orientation having a lower wall superheat. The boiling curve for the horizontal, downward-facing position ($\theta = -90$ degrees) showed much larger wall superheats than for either

0 or 90 degrees, and CHF was several times smaller. Githinji and Sabersky only studied the three cardinal angles, thus precluding their ability to find an optimal angle between 0 and -90 degrees. Class et al. (1959) examined the pool boiling of liquid hydrogen at 0, 45, and 90 degree orientations. Wall superheat was lowest when the boiling surface was vertical.

In forced-convection boiling, flow direction with respect to gravity becomes important because of the drastic density difference between the vapor and liquid phases. Figure 1(b) illustrates the difference between upflow and downflow in a forced-convection boiling system. Both the bubbles and the liquid move in a direction which opposes gravity in stable upflow. In downflow, the bubbles may move with the liquid (with gravity) or against the liquid (opposing gravity) depending upon the liquid velocity. Simoneau and Simon (1966) examined the forced-convection boiling of nitrogen in a vertical channel which was heated on one side. The nitrogen inlet velocity was varied from 25.9 to 106.7 cm/s for both upflow and downflow. The major differences observed for downflow as compared to upflow were changes in the bubble trajectories from countercurrent for low velocities to co-current for high velocities, larger vapor accumulation in the channel, and decreased CHF at low velocities. Higher liquid velocities lessened the vapor accumulation and the decrease in CHF as conditions more closely resembled those of upflow due to the diminished effect of buoyancy.

Mishima and Nishihara (1985) studied the effects of upflow and downflow of water at low velocities on CHF in a long rectangular channel. The cross section of the channel was $2.4 \times 40 \text{ mm}^2$ which was heated on either one or two of the 40 mm sides. For extremely small flow rates, CHF was triggered by flooding in both upflow and downflow. As the flow rate was increased for the upflow conditions, annular flow appeared in the downstream portion of the channel. Critical heat flux for these conditions increased with increasing flow rate. As the flow rate was increased for downflow, a critical mass velocity was reached at which the drag force of the incoming liquid on the bubble equalled the buoyancy force, causing the bubbles to stagnate in the channel; this triggered CHF at an even lower heat fluxes than for flooding. Increasing flow rate above the critical value in downflow forced bubbles to be entrained with the flow and increased critical heat flux. The data of Mishima and Nishihara show that because of flooding and other two-phase instabilities, CHF in a forced-convection boiling system with a small flow rate may be considerably lower than CHF in pool boiling.

The present paper will address the effects of channel orientation on nucleate boiling and CHF of Fluorinert FC-72 from a series of nine in-line, discrete heat sources simulating a multi-chip electronic module. The primary objective of this study is to guide the packaging engineer in the design of forced-convection boiling systems and to illustrate the sensitivity of such systems to circuit board orientations.

Experimental Apparatus

Flow Loop. A two-phase flow loop was constructed in

Nomenclature

g = gravitational constant
 k = thermal conductivity
 L = chip length in flow direction (10 mm)
 \overline{Nu}_L = average Nusselt number based on chip length
 Pr = Prandtl number
 P = pressure
 q'' = wall heat flux

q''_m = critical heat flux
 Re_L = Reynolds number based on chip length, UL/ν
 T = temperature
 ΔT_{sub} = inlet liquid subcooling, $T_{sat} - T_{f,in}$
 ΔT_w = temperature gradient between the chip surface and inlet liquid, $T_w - T_{f,in}$

U = mean inlet liquid velocity
 ν = dynamic viscosity
 θ = orientation angle measured from the vertical position

Subscripts

f = liquid
 in = inlet to multi-chip module
 sat = saturated
 w = mean chip surface condition

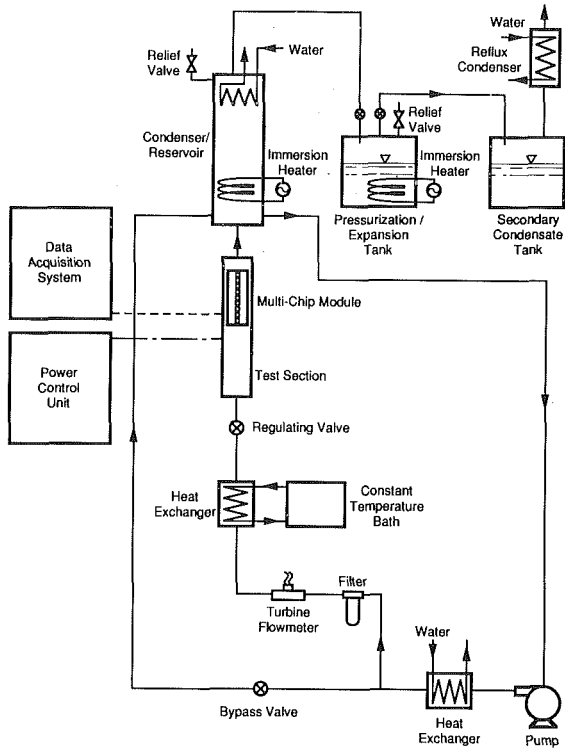


Fig. 2 Flow loop

order to condition the FC-72 fluid to the desired inlet test section velocity, temperature, and pressure. As shown in Fig. 2, the fluid was circulated in the loop by a magnetically coupled, centrifugal pump. In order to maintain flow stability, only a fraction of the total flow entered the test section while the rest was routed through a bypass line. Fluid velocity in the test section was controlled by two regulating valves, one located in the bypass line and the other just upstream of the test section. The flow rate of the test section fluid was measured by one of two turbine flowmeters depending on the flow rate. Inlet fluid temperature was maintained by two heat exchangers. The first heat exchanger, located immediately downstream of the pump, was used to cool the bulk flow from energy supplied to the flow by either the simulated chips or pipe friction. The second heat exchanger was located downstream of the turbine flowmeters to fine tune the fluid temperature prior to entering the test section. Upon exiting the test section, the fluid entered the condenser/reservoir where it recombined with the fluid from the bypass line; the mixture then returned to the pump.

Pressure was measured along the channel cover facing the most upstream chip in the array, and the differential pressure was measured between the most upstream and most downstream chips. In order to prevent air leaks into the system, the pressure at the most upstream chip was maintained at 1.36 bar (20 psi) for all of the experiments. The condenser/reservoir and the pressurization/expansion tank were used to keep the system pressure to within ± 0.0103 bar (± 0.15 psi) by means of a submerged water-cooled condenser and two immersion heaters as shown in Fig. 2.

The test section, Fig. 3, was comprised of the flow channel, upstream and downstream reservoirs, and multi-chip module. The test section was attached to a support frame which was fabricated to allow for rotation in increments of 45 degrees. A honeycomb section in the upstream reservoir served to straighten the flow and break up large turbulent eddies. Convergence of the flow to the channel dimensions of 20.0 mm \times 5.0 mm was achieved in the upstream reservoir. The flow was hydrodynamically developed in the remainder of the channel before it reached the chips. The most upstream edge of the

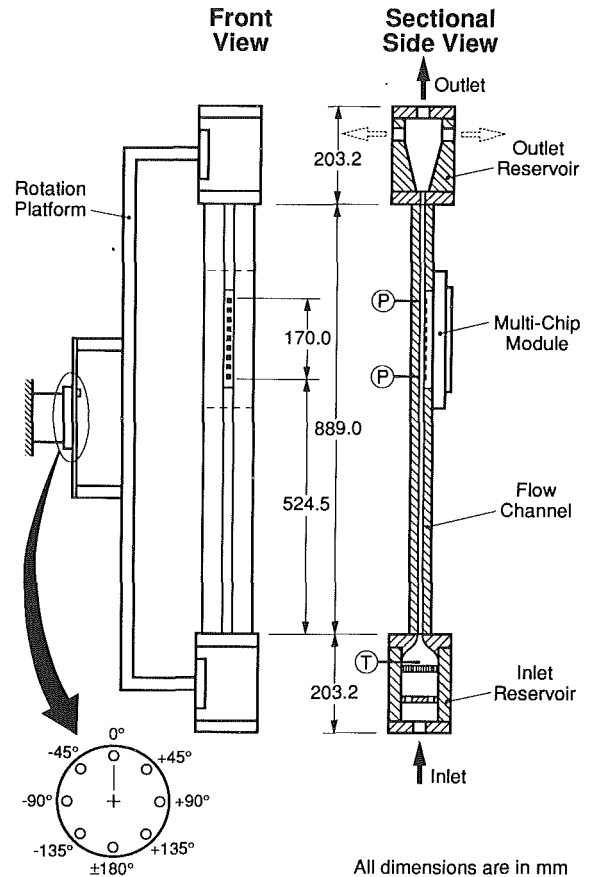


Fig. 3 Schematic of test section

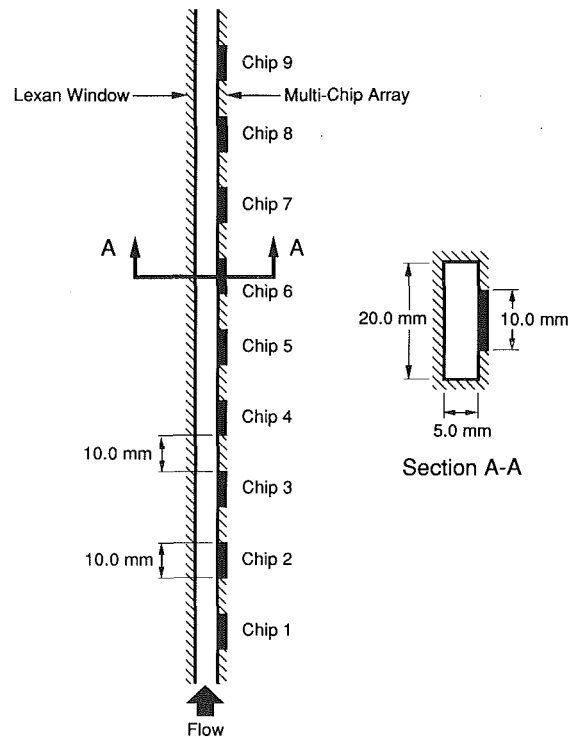


Fig. 4 Cross-sectional view of the channel and multi-chip array

first chip was 524.5 mm downstream of the upstream reservoir. The rest of the chips were positioned linearly downstream of the first chip at a pitch of 20.0 mm as shown in Fig. 4. A Lexan window, which housed the pressure taps, served as the

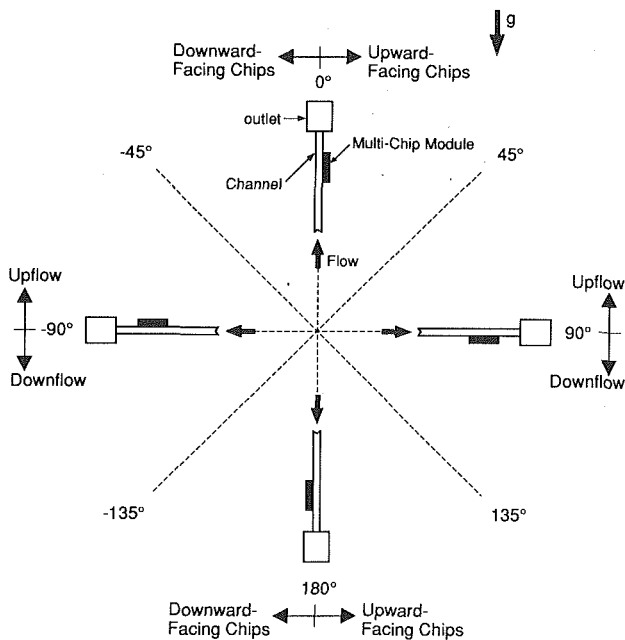


Fig. 5 Nomenclature for the angle of orientation

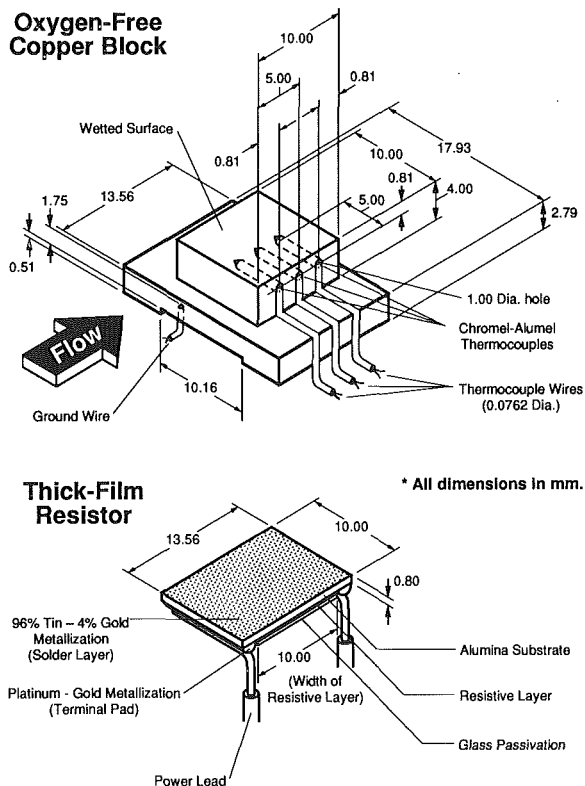


Fig. 6 Simulated microelectronic chip

top cover for the channel, and the multi-chip module formed the opposite wall at the location of the chips. To facilitate the removal of vapor from the test section at all of the angles tested, three exit ports were drilled at the downstream end and on opposing sides of the downstream reservoir.

To identify specific chips within the array, a nomenclature was established that refers to Chip 1 as the most upstream chip in the array as shown in Fig. 4. The remaining chips were sequentially assigned numbers up to nine. Figure 5 illustrates the nomenclature used to describe the angle of orientation.

The 0-degree reference was taken to be the vertical position with the fluid flow opposing gravity (upflow). The angle increases from 0 as the test section rotates in both directions with positive angles referring to orientations in which the chip surfaces were upward facing with respect to gravity, and negative angles to orientations in which the chip surfaces were downward facing.

Heat Source Design. As shown in Fig. 6, the simulated chip was machined from an oxygen-free copper block such that the cross-sectional dimensions of the chip surface in contact with the fluid were $10.0 \times 10.0 \text{ mm}^2$. A thick-film resistor of approximately 91Ω was soldered to the underside of the copper block. Three Chromel-Alumel thermocouples were instrumented into the copper block at a depth of 0.81 mm below the boiling surface. The thermocouples were aligned in the center of the chip along the flow direction at 0.81, 5.00, and 9.19 mm from the leading edge. One-dimensional heat conduction was used to calculate the surface temperature above each of the three thermocouples, and a weighted average of the three surface temperatures was taken to determine the mean surface temperature.

During the experiments, a parallel electrical circuit powered the nine thick-film resistors. In order to make each chip dissipate heat at the same rate, nine variable resistors were installed and adjusted in each leg of the circuit to alter the current to each chip. Since the voltage across each chip was the same, only one voltage transducer and nine current transducers were needed to measure the power dissipation of each chip. The data acquisition system independently shut off the electric power input to each chip once that chip had reached CHF. This not only saved each chip from burnout but also allowed the tests to continue until each chip reached CHF.

Operating Procedure. To ensure uniformity between the tests, the chip surfaces were vapor blasted with a water-particulate slurry having an average particle size of $10 \mu\text{m}$. Each time the system was started, the flow loop was deaerated for twenty minutes prior to taking any data. The procedure for obtaining data was to rotate the test section to the desired angle and then take all of the data for the desired ranges of velocity and subcooling before rotating the channel to a new angle. The standard daily procedure was to start with a particular subcooling and vary the velocity. Repeatability data were taken daily and checked with previous data obtained at the prescribed angle, and repeatability checks at previous angles were also performed occasionally.

Data Acquisition. A Keithley 500 series data acquisition system and a Compaq microcomputer were used to collect the experimental data which included twenty-seven temperatures for the nine simulated chips, fluid temperature in the upstream reservoir, absolute pressure at Chip 1, differential pressure between Chip 1 and Chip 9, frequency of the turbine flowmeter, and the voltage outputs from the voltage and current transducers.

The fluid temperature at Chip 1 was measured with a thermocouple probe introduced into the flow through the Lexan window and was found to agree with the corresponding temperature in the upstream reservoir of the test section to within 0.2°C for all flow rates and subcoolings tested; hence, temperature was measured only in the upstream reservoir to avoid disrupting the flow at Chip 1 by the thermocouple probe.

The saturation pressure for the multi-chip array was taken to be the pressure at the most upstream chip. Inlet subcooling was then calculated as the difference between the corresponding saturation temperature and the fluid temperature in the upstream reservoir. Average fluid velocity in the channel was calculated from the flow rate measured by the turbine flowmeters.

Table 1 Experimental uncertainty

Experimental Reading	Experimental Uncertainty (\pm)	Method of Estimation
Thermocouple	0.2 °C	Manufacturer, Calibration
Heat Flux (voltage and current transducers)	0.43 W/cm ² at 5.7 W/cm ² 0.98 W/cm ² at 30.0 W/cm ² 1.96 W/cm ² at 120. W/cm ²	Calibration
Flowmeter ($U \leq 75$ cm/s)	0.13 cm/s	Manufacturer
Flowmeter ($U > 75$ cm/s)	2.68 cm/s	Manufacturer
Absolute Pressure	0.0103 bar (0.15 psi)	Manufacturer
Differential Pressure	0.0103 bar (0.15 psi)	Manufacturer

A data point was accepted only after the entire system attained steady-state. For almost all of the tests, steady-state was reached when all of the chip temperatures and the upstream reservoir temperature had a standard deviation of less than 0.1°C for twenty consecutive readings over a period of 20 s. At some orientations, the chip temperatures near CHF oscillated by as much as $\pm 1.5^\circ\text{C}$ during low-velocity tests. For these tests, steady state was assumed when the oscillations became steady and repeatable over several sets of twenty temperature readings. Care was taken to ensure that CHF was not reached prematurely because of a large increment in power. Near CHF, the heat flux increments were decreased to 0.5 W/cm². As a standard, CHF was taken to be the last stable heat flux plus one half of the last power increment (~ 0.25 W/cm²). A large and rapid increase in the chip temperature signalled the attainment of CHF.

Experimental Uncertainty. The maximum uncertainty associated with each experimental reading is given in Table 1. The parameters in the one-dimensional heat conduction adjustment introduced a maximum uncertainty of $\pm 0.1^\circ\text{C}$ in the chip surface temperature. A two-dimensional numerical analysis was performed in order to calculate the percentage of the energy dissipated by the thick-film resistor which did not get conducted to the fluid/chip interface. By accounting for the additional surface area of the three-dimensional chip and neglecting any contact resistances, the largest heat loss for all experiments was calculated to be 3 percent. Due to the small heat losses, no correction was made to the power dissipated by the thick-film resistor in determining the chip heat flux. Table 2 details overall uncertainties in measuring the important parameters presented in this paper using the propagation of error suggested by Moffat (1988).

Results and Discussion

Single-phase, nucleate boiling, and critical heat flux (CHF) data were taken for each of nine chips for eight orientations at 45-degree increments. At each angle, the flow velocity was varied between 13 and 400 cm/s for subcoolings of 3, 14, 25, and 36°C and an inlet pressure of 1.36 bar. Data for the 0-degree orientation were reported by Willingham and Mudawar (1992).

Single-Phase Results. Flow in the channel was assumed to be fully turbulent because the Reynolds number based on the

Table 2 Overall uncertainties

Parameter	\pm % of value (max)
U	1.0 ($U \leq 75$ cm/s) 2.7 ($U > 75$ cm/s)
L	0.13
Single Phase	
ΔT	3.64
q''	7.47
Re_L^*	1.0 ($U \leq 75$ cm/s) 2.7 ($U > 75$ cm/s)
$\overline{Nu}_L / Pr^{1/3}^*$	8.3
Two Phase	
ΔT	3.64
q''	< 3.26

* Not including uncertainties in fluid properties.

channel hydrodynamic diameter was greater than 2832 for all of the test parameters; ninety-five percent of the data points had Reynolds numbers greater than 10,000. Figure 7 shows the average Nusselt numbers for Chips 1, 4, and 9 for all angles, velocities, and subcoolings, plotted with respect to Reynolds number based on the chip length. The Nusselt number was calculated from the measured heat flux and wall-to-fluid temperature difference,

$$\overline{Nu}_L = \left(\frac{q''}{T_w - T_{f,in}} \right) \frac{L}{k_f} \tag{1}$$

All of the fluid properties used in reducing the data for Fig. 7 and Eq. (1) were evaluated at the inlet temperature. Using the inlet fluid temperature has the added benefit of being a convenient design parameter for electronic packaging.

The Nusselt number was also referenced to the inlet temperature for all of the chips because of the small stream-wise temperature increase of the bulk fluid. A simple energy balance on the fluid resulted in a maximum stream-wise temperature increase of 1.5°C for low-velocity, highly-subcooled cases and 1.0°C for low-velocity, near-saturated cases. Because the wall-to-inlet fluid temperature difference became large as heat flux increased in highly-subcooled flow, the error associated with neglecting bulk fluid warming is negligible for these cases. With near-saturated flow, the maximum error associated with neglecting the warming of the bulk fluid was found to be 7 percent. The addition of this uncertainty into the calculation of $\overline{Nu}_L / Pr^{1/3}$ would increase its overall uncertainty to ± 13.1 percent. Data for the lowest flow rate, 13 cm/s, show the most scatter which might be attributed to the relatively large ex-

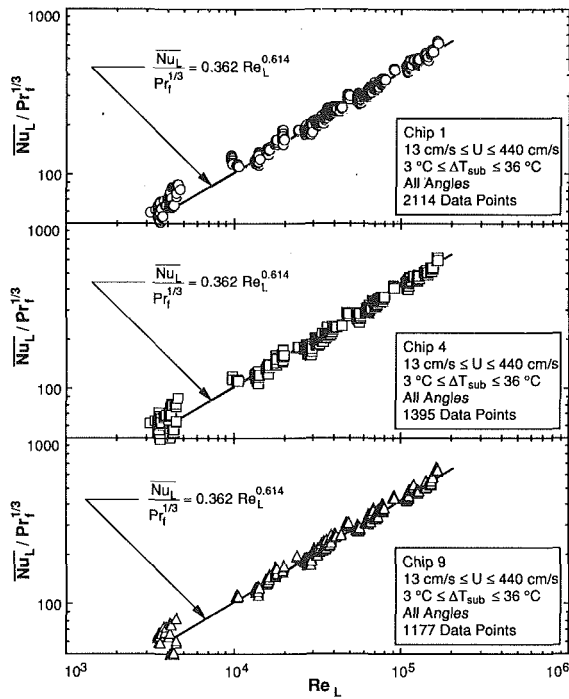


Fig. 7 Single-phase heat transfer data for Chips 1, 4, and 9 at all experimental conditions

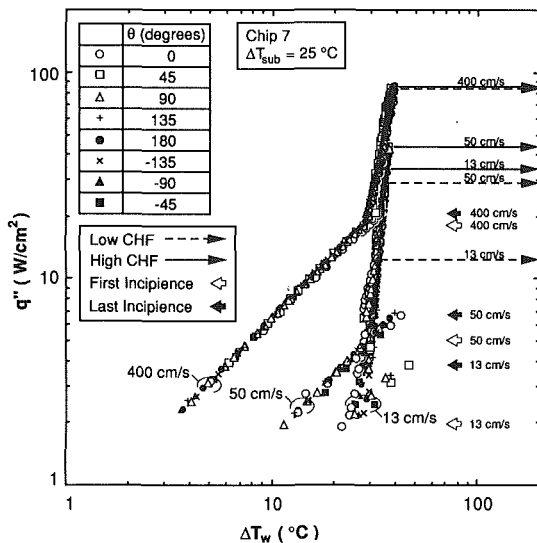


Fig. 8 Velocity effect on the boiling curve of Chip 7 at an inlet subcooling of 25°C

perimental error in the lower heat fluxes and flow rates (Table 2) or, potentially, to mixed convection effects. A least squares power law fit, given in Eq. (2), was used to correlate the data for all nine chips and at all of the test parameters with a mean absolute error for the 12,399 data points of 5.08 percent.

$$\frac{\overline{Nu}_L}{Pr_f^{1/3}} = 0.362 Re_L^{0.614} \quad (2)$$

Although other correlations have been made for discrete heat sources in a flow channel (e.g., Maddox and Mudawar, 1989; Samant and Simon, 1989; Incropera et al., 1986), the present data are not compared to these correlations because of differences in the respective hydraulic diameters of the flow channels. Unlike a continuous heated strip for which the single-phase heat transfer coefficient changes in the stream-wise direction, the simulated chips all had similar heat transfer

coefficients suggesting the non-heated space between chips may serve to reinitiate the thermal boundary layer at each chip. Details of these single-phase heat transfer phenomena are beyond the scope of this paper.

Effects of Orientation on Nucleate Boiling. The effects of velocity and orientation on the nucleate boiling curve are shown in Fig. 8 for Chip 7 at $\Delta T_{sub} = 25^\circ\text{C}$. Since the parametric trends in nucleate boiling were fairly similar for all nine chips, the following discussion will focus on a single chip, Chip 7. At each velocity, the boiling curves for all of the angles fall on top of one other, with a maximum temperature difference at constant heat flux of about 4°C with the exception of incipient boiling, which was promoted by some angles at a smaller wall superheat than other angles, and the pre-CHF region. Contrary to the findings of earlier pool boiling investigations, the effect of orientation on the wall temperature did not follow a clear trend. Perhaps in forced-convection boiling the growing bubbles are sheared from the wall by the bulk fluid rather than being removed by buoyancy forces. As a result, the change in orientation does not have as much of an impact on bubble departure as it does in pool boiling. As shown in Fig. 8, increased velocity increased the single-phase heat transfer coefficient, delayed boiling incipience to higher fluxes, and increased CHF. The range of incipient heat fluxes for each velocity is shown bound by an open and a solid arrow. Near CHF, the boiling curves for the three velocities are shown to coincide with each other, but unlike single-phase and nucleate boiling heat transfer, CHF was affected by orientation. The range of CHF values for each velocity is bound by a dashed and a solid arrow. At an inlet velocity of 400 cm/s, there is little effect of orientation on CHF as evidenced by the closeness of the two CHF arrows. The effect of orientation on CHF is discussed in more detail in the next section.

The effects of subcooling and orientation on the boiling curve for Chip 7 are illustrated in Figs. 9(a) and 9(b) for $U = 50$ and 400 cm/s, respectively. The successful dimensionless correlation of the single-phase data shown in Fig. 7 proves the slight scatter in the single-phase data in Figs. 9(a) and 9(b) is due to the changes in fluid properties associated with the different inlet temperatures. Increased subcooling delayed nucleate boiling and CHF to higher heat fluxes for both low and high velocities, as shown in Figs. 9(a) and 9(b), respectively. At each subcooling, the boiling curves for all the angles fall on top of each other with a maximum temperature deviation of 6°C except during incipience even though the logarithmic plot makes the boiling curves appear to group more tightly at higher subcoolings. Occasionally for low-subcooled flow at $U = 400$ cm/s, some of the chips would gradually slip into nucleate boiling by boiling over only a small portion of its surface area. This served to lower the wall temperature in steps as more of the surface began to boil. The effect of orientation on CHF decreased slightly with increased subcooling as evidenced by comparing the low and high CHF values in Fig. 9(a), and high velocities almost completely dampened the CHF sensitivities to orientation as shown in Fig. 9(b). Trends in the effects of velocity on the single-phase heat transfer and subcooling on nucleate boiling heat transfer for all the orientations considered in the present study are similar to those for vertical upflow as reported by Willingham et al. (1991) and Willingham and Mudawar (1992). That is, the two most upstream chips in the multi-chip array were the only chips to experience a significant temperature drop at the incipience of boiling, and increases in ΔT_{sub} decreased the wall superheat, but the actual magnitude of the temperature drop depended on the heat flux and the location of the chip in the multi-chip array. However, during nucleate boiling, the wall temperature did not decrease when velocity was increased as was reported by Willingham et al. This might be attributed to the difference in surface

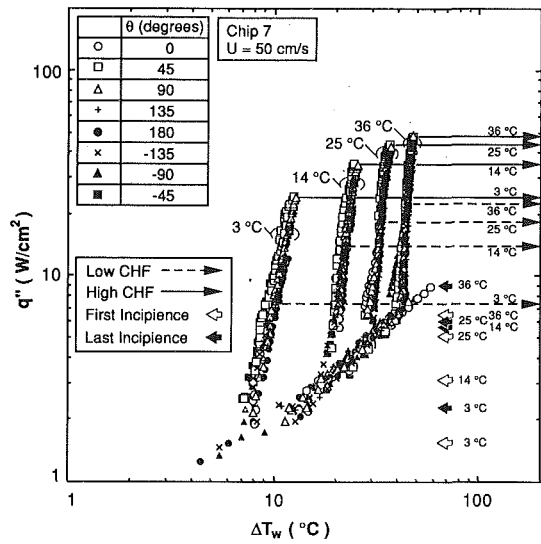


Fig. 9(a)

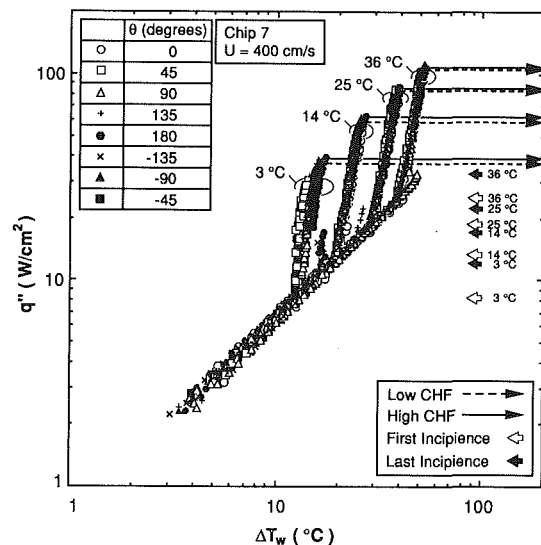


Fig. 9(b)

Fig. 9 Subcooling effect on Chip 7 for an inlet velocity of (a) 50 cm/s and (b) 400 cm/s

finish between the two studies; Willingham et al. employed chips with mirror-polished surfaces.

Minimum Critical Heat Flux in Multi-Chip Array. The minimum critical heat flux value in the multi-chip array is plotted with respect to velocity in Figs. 10(a) and 10(b) for $\Delta T_{sub} = 3$ and 25°C , respectively. From a design standpoint, the lowest CHF value in the array is of great significance since it determines when damage will first occur to the system. Most of the angles produced relatively similar CHF values; however, at lower velocities CHF decreased considerably for orientations which were subjected to downflow and where the chips were downward facing.

For near-saturated conditions, Fig. 10(a), the CHF values for $\theta = 180$ and -135 degrees show a minimum at ~ 25 cm/s. This may be explained by the observed bubble movement relative to the bulk flow. At $u = 13$ cm/s, bubbles were observed to move upstream (opposite of the liquid flow) and condense upstream of Chip 1. This bubble movement helped mix the flow and cause more liquid to come into contact with the wall, thus increasing CHF. Occasionally, long vapor bubbles, which resemble those encountered in two-phase slug flow,

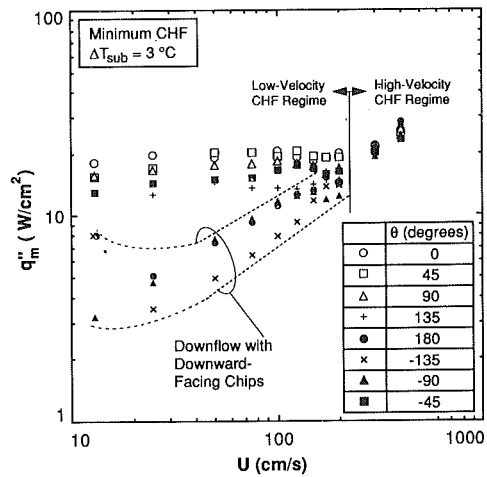


Fig. 10(a)

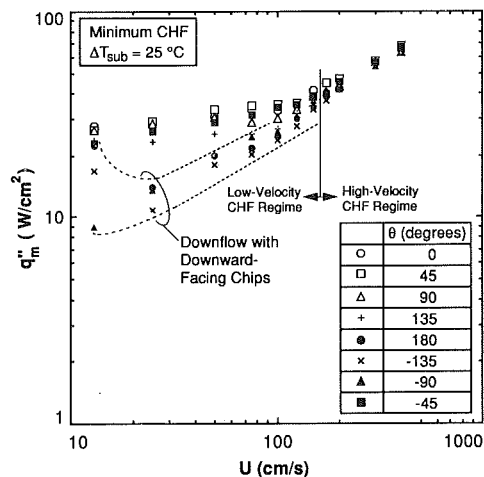


Fig. 10(b)

Fig. 10 Velocity effect on the minimum critical heat flux in the multi-chip array for an inlet subcooling of (a) 3°C and (b) 25°C

were observed to propagate in the channel primarily over the most upstream chips; these bubbles were not observed to starve the chip surface from liquid for any appreciable length of time. Although the opposing vapor flow served to increase CHF in the present large scale flow loop, an electronic cooling system should not be designed to operate with counterflow because of the many two-phase instabilities which could affect the system performance, especially if such a system is to adhere to the stringent volume constraints of electronic packaging. Some of the possible problems in miniaturized two-phase loops are density wave instabilities and pressure oscillations resulting from the momentary cessation of liquid flow due to vapor blockage and vapor trapping in the loop high-spots.

At 25 cm/s (401 kg/m²s), the bubbles sometimes remained stagnant over the chips for $\theta = 180$ and -135 degrees, causing CHF to decrease due to dryout at the chip surface. Since no other velocities between 13 and 50 cm/s were tested, a precise range for stagnation could not be obtained. Mishima and Nishihara (1985) found bubble stagnation in water flow to take place at mass velocities between 150 and 200 kg/m²s. Differences in stagnation mass velocities between the two studies are to be expected due to the large differences in thermal and interfacial properties between FC-72 and water and to the discontinuities of wall heat flux in the present study. For velocities greater than 50 cm/s in the present study, the bubbles were observed to exit the channel with the liquid flow at all orientations.

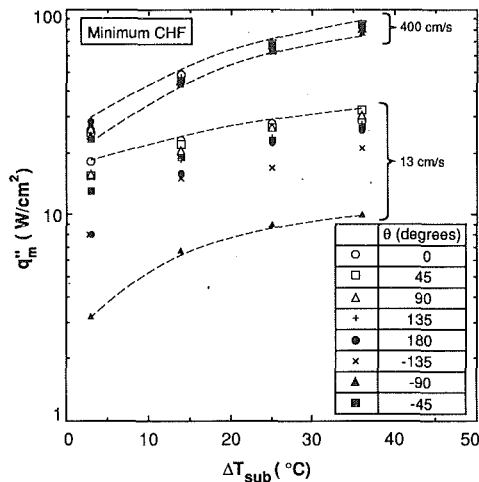


Fig. 11 Subcooling effect on the minimum critical heat flux in the multi-chip array for an inlet fluid velocity of 13 and 400 cm/s

For $\theta = -90, -45, 0, 45,$ and 90 degrees, the bubbles always exited the channel with the bulk flow. At $\theta = 90$ and -90 degrees, during the low-velocity tests, the bubbles appeared to rise through the bulk fluid forming stratified flow. From an application standpoint, flow stratification is a cause for concern since the vapor can develop a much higher velocity than the liquid (Dukler and Taitel, 1986). Large velocity differences between the two phases promote waviness in the vapor-liquid interface and may cause a Helmholtz instability resulting in plug flow and undesirable pressure oscillations. At $\theta = 135$ degrees, vapor counterflow and stagnation were observed for $U = 13$ and 25 cm/s, respectively. The CHF did not decrease as much for this angle as it did for $\theta = 180$ and -135 degrees, because the chips were upward-facing, and the vapor could easily move away from the chip surface. This allowed liquid to stay in contact with the heated surface; eventually though, the large void fraction in the channel caused CHF to occur at a lower value than for vertical upflow where bubbles were carried out of the test section. Again at $\theta = 90$ and 135 degrees there is the potential for vapor trapping inside actual electronic cooling systems.

Figure 10(a) shows that the effect of orientation on the minimum CHF value was virtually non-existent for velocities greater than 200 cm/s as the CHF values converged. This implies the high velocity of liquid was sufficient to both force vapor bubbles to be entrained along and to replenish the chip surfaces with liquid even in the downward-facing orientations.

Similar observations may be made for the minimum CHF values in the multi-chip array at $\Delta T_{sub} = 25^\circ\text{C}$. Figure 10(b) shows most of the orientations have CHF values which are close to each other with the exception of angles with downflow and downward-facing chips. At these angles, 180 and -135 degrees, the bubbles exhibited similar hydrodynamic behavior as they did with $\Delta T_{sub} = 3^\circ\text{C}$. The CHF values converged for all orientations for velocities exceeding 150 cm/s, which is lower than for near-saturated flow.

There appears to be a change in slope in the CHF data in Figs. 10(a) and 10(b) marking a transition between low-velocity and high-velocity CHF regimes. Mudawar and Maddox (1989) observed a similar transition which coincided with a change in the CHF mechanism for their single chip experiments in vertical upflow. Low-velocity CHF was observed to result from a large vapor blanket over the entire surface of the chip causing dryout, and high-velocity CHF was triggered by surface dryout at localized vapor patches on the surface.

Figure 11 shows the effect of subcooling on the minimum CHF values for $U = 13$ and 400 cm/s. For the lower of the two velocities, the CHF values at the various angles were sim-

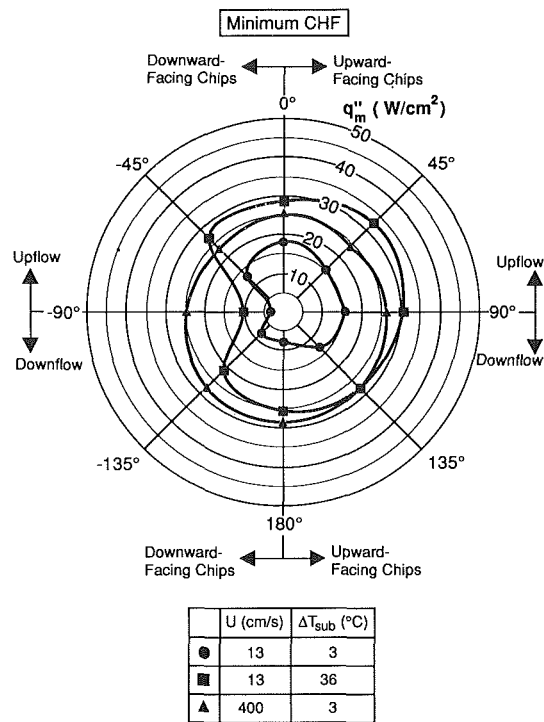


Fig. 12 Polar representation of velocity and subcooling effects on the minimum critical heat flux value in the multi-chip array

ilar, except for angles with downflow and downward-facing chips. For all velocities, increasing ΔT_{sub} was observed to both increase CHF and reduce the spread in CHF due to orientation. Apparently, the larger bubbles and higher void fractions at near-saturated conditions rendered certain orientations more detrimental, especially for downflow. As shown in Fig. 11, CHF was lowest for all four subcoolings at $\theta = -90$ degrees; for $\Delta T_{sub} = 3, 14, 25,$ and 36°C , those CHF values were, respectively, 17.8, 29.5, 32.5, and 35.3 percent of the corresponding CHF for $\theta = 0$ degree (vertical upflow). Generally, the greatest deterioration in CHF occurred for low velocities and low subcoolings. Figure 11 shows a convergence of CHF values for 400 cm/s. For $\Delta T_{sub} = 3, 14, 25,$ and 36°C , the lowest CHF values attained at 400 cm/s for the four subcoolings were, respectively, 89.9, 91.3, 98.3, and 92.2 percent of the corresponding value for vertical upflow. Therefore, in an electronic cooling system, the effects of orientation can be overcome but at the expense of increased pumping requirements.

In order to illustrate a portion of the aforementioned results, a polar plot of some of the minimum CHF data is presented in Fig. 12. For the case of lowest velocity, 13 cm/s, and lowest subcooling, 3°C , there is a decrease in CHF with increasing θ , culminating with the largest decrease at -90 degrees. For the same velocity but with $\Delta T_{sub} = 36^\circ\text{C}$, the decrease in CHF was much less for upward-facing chips, but CHF still decreased sharply for downflow and downward-facing chips. For comparison, data for the highest velocity, 400 cm/s, and lowest subcooling, 3°C , Fig. 12, show very little change in CHF with orientation.

Critical Heat Flux Bandwidth of the Multi-Chip Array. For each set of test conditions ($U, \Delta T_{sub}$, and θ), the heat fluxes at which the nine simulated chips reached CHF were recorded. From these values, a CHF bandwidth was calculated for the chip array according to the relation

$$\text{CHF Bandwidth } (\pm \%)$$

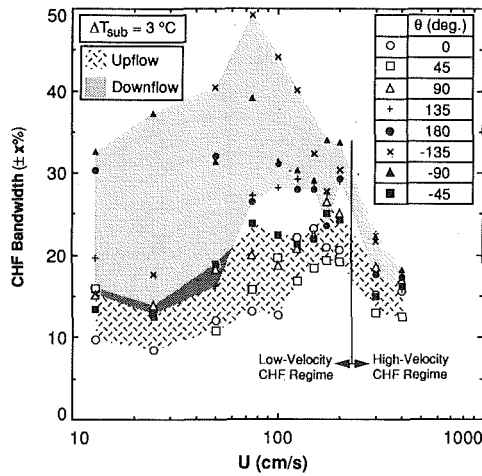


Fig. 13(a)

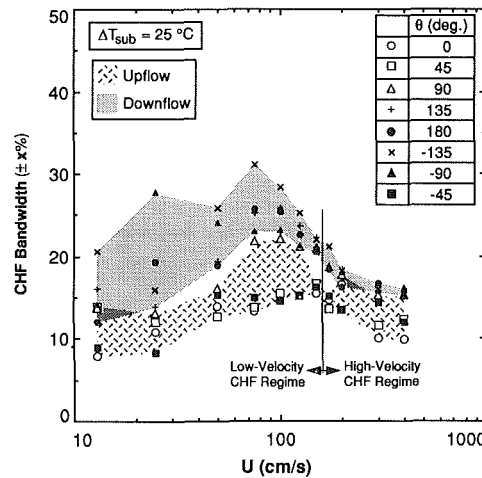


Fig. 13(b)

Fig. 13 Bandwidth of critical heat flux values for all angles of orientation for an inlet subcooling of (a) 3°C and (b) 25°C

$$= \frac{(\text{Maximum CHF} - \text{Minimum CHF})}{\frac{1}{2}(\text{Maximum CHF} + \text{Minimum CHF})} \times (\pm 50 \text{ percent}) \quad (3)$$

This bandwidth reflects the relative spread in CHF data for the array of chips at the particular test conditions and should not be confused with the spread in CHF data caused by changes in orientation shown in Figs. 8, 9(a), and 9(b). The maximum CHF value corresponds to the last chip to progress to film boiling after all of the other chips had already reached CHF and had their power cut off.

The CHF bandwidths are plotted in Figs. 13(a) and 13(b) against velocity for $\Delta T_{\text{sub}} = 3$ and 25°C, respectively. Each angle is designated with its own symbol, and the range of bandwidths for upflow and downflow conditions have been shaded. Although orientations of ± 90 degrees correspond to horizontal flow and not upflow or downflow, data for $\theta = +90$ degrees have been lumped with the upflow cases since they share similar CHF trends. Likewise, data for $\theta = -90$ degrees have been combined with the downflow cases. Figures 13(a) and 13(b) show downflow orientations produced considerably larger bandwidths. Bandwidths for both upflow and downflow decreases considerably in the high-velocity CHF regime. Increased fluid subcooling also decreased the CHF

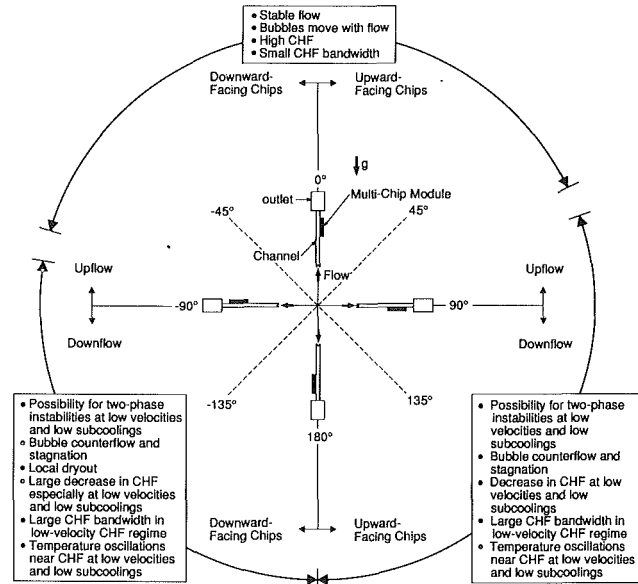


Fig. 14 General trends in the effects of orientation on cooling performance

bandwidth as evidenced by comparing Figs. 13(a) and 13(b). The relatively small bandwidths attained with vertical upflow make this orientation very attractive for cooling where cooling uniformity in the chip array is a prime concern.

Overall Effects of Orientations. A summary of the general orientation trends observed during this study is given in Fig. 14. The angles are divided into three groups. The first group encompasses $\theta = -45, 0,$ and 45 degrees. This group overwhelmingly outperformed the rest of the angles in flow stability, absolute CHF value, and CHF uniformity between the chips; they should therefore be the angles of choice for a two-phase cooling system. The second group includes $\theta = 90$ and 135 degrees. These two angles did not perform well under low-velocity and low-subcooling conditions and are candidates for two-phase instabilities. The last group of angles, $\theta = 180, -135,$ and -90 degrees, performed the worst and should be avoided when designing a two-phase cooling system. These angles all resulted in significantly reduced values of CHF especially at low velocities and low subcoolings.

Conclusions

The effect of orientation angle on the forced-convection boiling and CHF of FC-72 from a linear array of nine, in-line simulated microelectronic chips was investigated. The following conclusions can be made:

- (1) Changes in orientation produced in significant variations in the single-phase heat transfer coefficient for all the conditions tested. Nucleate boiling was also not affected by orientation.
- (2) For each individual orientation, increased velocity was observed to increase the single-phase heat transfer, delay the incipience of nucleate boiling to higher heat fluxes, and increase CHF. Increased subcooling was also observed to delay the incipience of nucleate boiling and increase CHF.
- (3) For liquid velocities below 200 cm/s, the lowest CHF values were measured for downward-facing chips subjected to downflow ($\theta = 180, -135,$ and -90 degrees). At these angles, the lowest CHF occurred when the bubbles stagnated on the chip surface causing premature dryout. For liquid velocities below 200 cm/s, the highest CHF values were measured for upflow with the

chips either upward or downward facing ($\theta = -45, 0, 45$ degrees).

- (4) Critical heat flux was not affected by orientation for inlet fluid velocities greater than 200 cm/s for near-saturated flow. Increased subcooling dampened the effect of orientation and allowed for operation insensitive to orientation at velocities as small as 150 cm/s.
- (5) For each velocity, subcooling, and orientation, CHF bandwidth in the multi-chip array was largest in the low-velocity CHF regime, and decreased sharply in the high-velocity CHF regime. Subcooling the liquid was found to decrease the CHF bandwidth for all velocities. The largest bandwidths were measured for downward-facing chips with downflow.
- (6) Upflow was found to be the orientation of choice for packaging multi-chip modules in two-phase cooling systems to insure consistent boiling, high CHF, and stable flow.

Acknowledgments

Support of this work by a grant from the Industrial Chemical Products Division of 3M is gratefully acknowledged.

References

- Anderson, T. M., and Mudawar, I., 1989, "Microelectronic Cooling by Enhanced Pool Boiling of a Dielectric Fluorocarbon Liquid," *ASME Journal of Heat Transfer*, Vol. 111, pp. 752-759.
- Chen, L. T., 1978, "Heat Transfer to Pool-Boiling Freon from Inclined Heating Plate," *Letters in Heat and Mass Transfer*, Vol. 5, pp. 111-120.
- Class, C. R., DeHaan, J. R., Piccone, M., and Cost, R. B., 1959, "Boiling Heat Transfer to Liquid Hydrogen from Flat Surfaces," *Advances in Cryogenic Engineering*, ed., K. D. Timmerhaus, Vol. 5, Plenum Press, New York, pp. 254-261.
- Dukler, A. E., and Taitel, Y., 1986, "Flow Pattern Transitions in Gas-Liquid Systems: Measurement and Modeling," *Multiphase Science and Technology*, eds., G. F. Hewitt, J. M. Delhay, and N. Zuber, Vol. 2, Hemisphere Publishing Corp., New York, pp. 1-94.
- Githinji, P. M., and Sabersky, R. H., 1963, "Some Effects of the Orientation of the Heating Surface in Nucleate Boiling," *ASME Journal of Heat Transfer*, Vol. 85, p. 379.
- Incropera, F. P., Kerby, J. S., Moffatt, D. F., and Ramadhyani, S., 1986, "Convection Heat Transfer from Discrete Heat Sources in a Rectangular Channel," *International Journal of Heat and Mass Transfer*, Vol. 29, pp. 1051-1058.
- Lee, T. Y., and Simon, T. W., 1989, "High-Heat-Flux Forced Convection Boiling from Small Regions," *Heat Transfer in Electronics 1989*, ed., R. K. Shah, ASME HTD-Vol. 111, pp. 7-16.
- Maddox, D. E., and Mudawar, I., 1989, "Single and Two-Phase Convective Heat Transfer from Smooth and Enhanced Microelectronic Heat Sources in a Rectangular Channel," *ASME Journal of Heat Transfer*, Vol. 111, pp. 1045-1052.
- McGillis, W. R., Carey, V. P., and Strom, B. D., 1991, "Geometry Effects on Critical Heat Flux for Subcooled Convective Boiling from an Array of Heated Elements," *ASME Journal of Heat Transfer*, Vol. 113, pp. 463-471.
- Mishima, K., and Nishihara, H., 1985, "The Effect of Flow Direction and Magnitude on CHF for Low Pressure Water in Thin Rectangular Channels," *Nuclear Engineering and Design*, Vol. 86, pp. 165-181.
- Moffat, R. J., 1988, "Describing the Uncertainties in Experimental Results," *Experimental Thermal and Fluid Sciences*, Vol. 1, pp. 3-17.
- Mudawar, I., and Anderson, T. M., 1989a, "High Flux Electronic Cooling by Means of Pool Boiling—Part 1: Parametric Investigation of the Effects of Coolant Variation, Pressurization, Subcooling, and Surface Augmentation," *Heat Transfer in Electronics 1989*, ed., R. K. Shah, ASME HTD-Vol. 111, pp. 25-34.
- Mudawar, I., and Anderson, T. M., 1989b, "High Flux Electronic Cooling by Means of Pool Boiling—Part 2: Optimization of Enhanced Surface Geometry," *Heat Transfer in Electronics 1989*, ed., R. K. Shah, ASME HTD-Vol. 111, pp. 35-49.
- Mudawar, I., and Maddox, D. E., 1989, "Critical Heat Flux in Subcooled Flow Boiling of Fluorocarbon Liquid on a Simulated Electronic Chip in a Vertical Rectangular Channel," *International Journal of Heat and Mass Transfer*, Vol. 32, pp. 379-394.
- Nakayama, W., Nakajima, T., and Hirasawa, S., 1984, "Heat Sink Studs Having Enhanced Boiling Surfaces for Cooling of Microelectronic Components," ASME Paper 84-WA/HT-89.
- Nishikawa, K., Fujita, Y., Uchida, S., and Ohta, H., 1983, "Effect of Heating Surface Orientation on Nucleate Boiling Heat Transfer," *Proceedings of the ASME-JSME Thermal Engineering Joint Conference 1983*, eds., Y. Mori and W. J. Yang, Vol. 1, Honolulu, Hawaii, pp. 129-136.
- Park, K. A., and Bergles, A. E., 1988, "Effects of Size of Simulated Microelectronic Chips on Boiling and Critical Heat Flux," *Journal of Heat Transfer*, Vol. 110, pp. 728-734.
- Park, K. A., Bergles, A. E., and Danielson, R. D., 1990, "Boiling Heat Transfer Characteristics of Simulated Microelectronic Chips with Fluorinert Liquid," *Heat Transfer in Electronic and Microelectronic Equipment*, ed., A. E. Bergles, Hemisphere Publishing Corp., New York, pp. 573-588.
- Samant, K. R., and Simon, T. W., 1989, "Heat Transfer from a Small Heated Region to R-113 and FC-72," *ASME Journal of Heat Transfer*, Vol. 111, pp. 1053-1059.
- Simoneau, R. J., and Simon, F. F., 1966, "A Visual Study of Velocity and Buoyancy Effects on Boiling Nitrogen," NASA, TN D-3354, Lewis Research Center, Cleveland, Ohio.
- Simons, R. E., 1987, "Direct Immersion Cooling: Past, Present, and Future," *IBM Technical Report*, TR 00.3465, International Business Machines Corp., Poughkeepsie, New York.
- Willingham, T. C., Gersey, C. O., and Mudawar, I., 1991, "Forced Convective Boiling from an Array of In-Line Heat Sources in a Flow Channel," *Proceedings of the ASME-JSME Thermal Engineering Joint Conference 1991*, eds., J.R. Lloyd and Y. Kurosaki, Reno, Nevada, Vol. 2, pp. 365-374.
- Willingham, T. C., and Mudawar, I., 1992, "Forced-Convection Boiling and Critical Heat Flux From a Linear Array of Discrete Heat Sources," *International Journal of Heat and Mass Transfer*, in press.